

Computational Intelligence in Electroencephalogram Analysis

Sude Pehlivan

Izmir Katip Celebi University

sudepehlivan35@gmail.com

12.11.2019

1 Introduction

- Brain
- Waves
- EEG
- Recording

2 Computational Intelligence in the Diagnosis of Neurological Disorders

- Epilepsy Detection
- Huntington's Disease Detection
- Alzheimer Detection
- Evoked Potentials

3 Brain Computer Interface

- 1 Brain is the control center of the nervous system which consists of building blocks called neurons.
- 2 Neurons process information in terms of electricity.
- 3 Electroencephalogram (EEG) machine is a device that records electrical activity of the brain either by invasive electrodes or by non-invasive surface electrodes.
- 4 First electrical activity of the brain was discovered by Richard Caton.
- 5 Hans Berger was the first man to amplify the electrical activity of the brain.

Computational intelligence in
biomedical engineering by Begg
et al.

EEG waves are sinusoidal and they can be separated by means of frequency. The amplitude interval of the EEG signal is between 0.5 to 100 micro volts which is peak to peak value. By analysing the power spectrum of the signal, one can observe 5 different frequency intervals as

- 1 Delta (up to 4 Hz)
- 2 Theta (4-8 Hz)
- 3 Alpha (8-12 Hz)
- 4 Beta (12-26 Hz)
- 5 Gamma (26-100 Hz)

Computational intelligence in
biomedical engineering by Begg
et al.

- ① 10-20 electrode placement system as a standard
- ② (F) frontal, (C) central, (O) occipital, (T) temporal and (P) posterior
- ③ Impedance must be lower than 5 K ohms

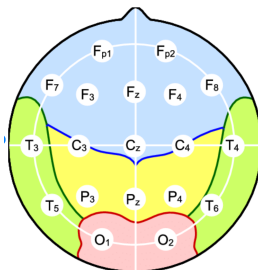


Figure: 10-20 System

Bos, D. O. (2006). EEG-based emotion recognition. The Influence of Visual and Auditory Stimuli, 56(3), 1-17.

An EEG system must be consist of

- ① Electrodes with conducting gel to receive signals
- ② Amplifiers to increase the amplitude of the signal
- ③ Filters to eliminate noise
- ④ A/D converter to provide readable digital data

Raw signal coming from the brain consists of the desired EEG data, artefacts such as biological signals, 50/60 Hz main voltage and noise.

Computational intelligence in
biomedical engineering by Begg
et al.

EPILEPSY

"Epilepsy is described as the excessive electrical discharge from brain cells"
or
"Repetitive high-amplitude activities" with fast, slow, or a combination of Spikes and Slow Waves (SSW)"

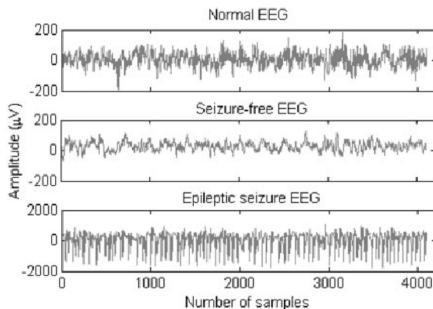


Figure: Epileptic Seizure EEG and Normal EEG Comparison

A Comparison of Algorithms for Detection of Spikes in the Electroencephalogram by Pang et al.

- ➊ Data was recorded through 24 hours with 8-channel EEG recorder
- ➋ F8-T4, T4-T6, T6-O2, F7-T3, T3-T5, T5-O1, C4-Cz, and Cz-C3 channels were selected
- ➌ Sample window of 2 s of the EEG data

DOI:10.1109/TBME.2003.809479

A Comparison of Algorithms for Detection of Spikes in the Electroencephalogram by Pang et al.

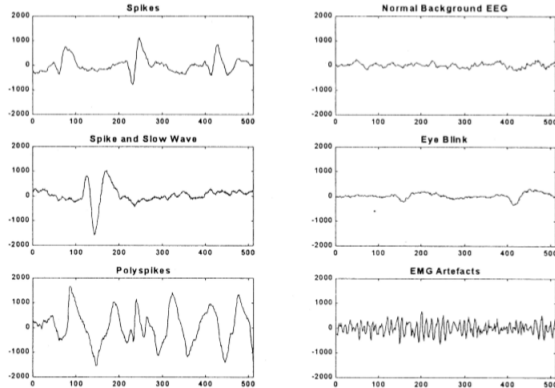


Figure: Spikes, Slow Waves and Artefacts

Tarassenko's Algorithm

- ① Uses both time and frequency domain parameters
- ② Average slope, Sharpness, Mobility and Complexity were used as time domain features.
- ③ AutoRegressive (AR) model parameters were used as frequency domain features

DOI:10.1109/TBME.2003.809479

Webber's Algorithm

- 1 Compresses the raw data and transforms it into context parameters
- 2 Neural network that transforms the context parameters into a smaller number of parameters
- 3 Rules that confirm the existence of the spike
Totally 31 context parameters were determined

DOI:10.1109/TBME.2003.809479

Kalayci's Algorithm

- 1 Enlarging the input window size of the classifier to improve performance
- 2 Wavelet transform was used with Daubechies-4 mother wavelet

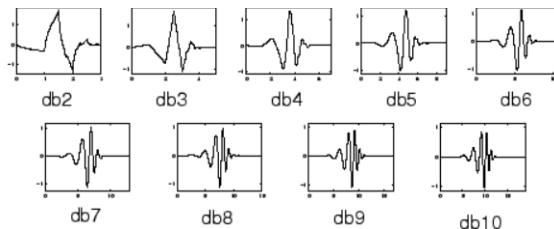


Figure: Daubechies Wavelets

- 1) **Sensitivity (SEN):** A measure of the ability of the classifier to detect spikes

$$\text{Sensitivity} = \frac{TP}{TP + FN} \times 100\%. \quad (5)$$

- 2) **Specificity (SPE):** A measure of the ability of the classifier to specify normal activities

$$\text{Specificity} = \frac{TN}{TN + FP} \times 100\%. \quad (6)$$

- 3) **Selectivity (SEL):** A measure of the ability of the classifier to reject false detections of spikes

$$\text{Selectivity} = \frac{TP}{TP + FP} \times 100\%. \quad (7)$$

- 4) **Average Detection Rate (ADR):** The average of sensitivity and specificity.

$$\text{Average detection rate} = \frac{\text{Sensitivity} + \text{Specificity}}{2} \times 100\%. \quad (8)$$

(a) Performance parameters

(Partial)	SEN	SPE	SEL	ADR
Tarassenko	86.78	93.88	81.65	90.33
Webber	90.05	93.02	80.88	91.53
Kalayci	86.21	94.89	83.93	90.55
Ozdamar	88.37	92.60	78.65	90.48

(a)

(Global)	SEN	SPE	SEL	ADR
Tarassenko	81.51	96.21	86.89	88.86
Webber	83.17	97.66	91.75	90.42
Kalayci	79.44	96.26	86.59	87.85
Ozdamar	80.40	96.36	87.04	88.38

(b) Performance

DOI:10.1109/TBME.2003.809479

Partial Training Method which selects three files and global training method which selects 2000 epochs were used to train.
Eight classifiers using different combinations of feature extraction algorithms and the above two training methods were used
They concluded no single method of spike detection is uniformly superior to all others

DOI:10.1109/TBME.2003.809479

Forecasting Generalized Epileptic Seizures from the EEG Signal by Wavelet Analysis and Dynamic Unsupervised Fuzzy Clustering by Geva and Kerem

- ① The elevated oxygen partial pressure induces generalized EEG seizure
- ② Existence of pre-Ictal State (PIS) generalized epilepsy was examined by Hyperbaric Oxygen (HBO) exposed rats.
- ③ Fronto-frontal and parieto-parietal regions were amplified, band-pass filtered between 1-30 Hz, notch-filtered at 50 Hz and divided into epochs.

DOI:10.1109/10.720198

$$\mathbf{S} = \begin{bmatrix} S(1) & S(D+1) & \cdot & \cdot & S((M-1) \cdot D + 1) \\ S(2) & S(D+2) & \cdot & \cdot & S((M-1) \cdot D + 2) \\ \cdot & \cdot & \cdot & \cdot & \cdot \\ \cdot & \cdot & \cdot & \cdot & \cdot \\ S(N) & S(D+N) & \cdot & \cdot & S((M-1) \cdot D + N) \end{bmatrix}$$

Figure: S Matrix

- ❶ N: Number of samples of each pattern vector
- ❷ M: Number of pattern vectors
- ❸ D: Delay of patterns

DOI:10.1109/10.720198

Fast Wavelet Transform (FWT), proposed by Mallat and Zhong was used.

- ① Each column of the time series matrix is decomposed into an orthogonal set of waveforms
- ② The simple biphasic mother wavelet was chosen
- ③ Convolve the signal with these dilated wavelets
- ④ The first five scales were chosen
- ⑤ Statistical values: the moments of variance (energy), skewness, and kurtosis of the wavelet coefficients, number of extrema per unit time
- ⑥ Unsupervised Optimal Fuzzy Clustering (UOFC) algorithm was used

DOI:10.1109/10.720198

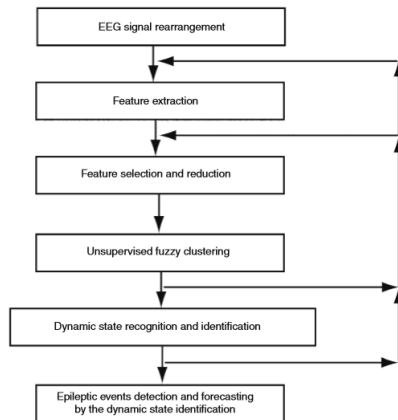


Figure: Method of Geva

Results were fluctuating but they were promising.

Epileptic Seizure Prediction Using Hybrid Feature Selection by D'allesandro et al.

- ① iEEG electrodes
- ② 3 to 14 days of continuous video-EEG monitoring
- ③ 0.1–100 Hz bandpass filter, 60-Hz notch filter
- ④ 46 preictal records, and 160 h of baseline data
- ⑤ 4 h of baseline data for training and 40 h for testing
- ⑥ Artificially generated data

DOI:10.1109/TBME.2003.810706

First Level of Features

- ① Curve length
 - ② Energy
 - ③ Nonlinear Energy
 - ④ Spectral Entropy (SE)
 - ⑤ Sixth Power
 - ⑥ Energy of the Wavelet Packets
- Second and Third Level of Features

- ⑦ Minimum
- ⑧ Maximum
- ⑨ Median
- ⑩ Mean
- ⑪ Variance
- ⑫ Standard deviation

Chromosome is the possible solution and it include “genes”

There are 4 “genes” in this paper:

- 1 Channels
- 2 First-level features
- 3 Second-level features
- 4 Third-level features

DOI:10.1109/TBME.2003.810706

Genetic Algorithm for Feature Selection

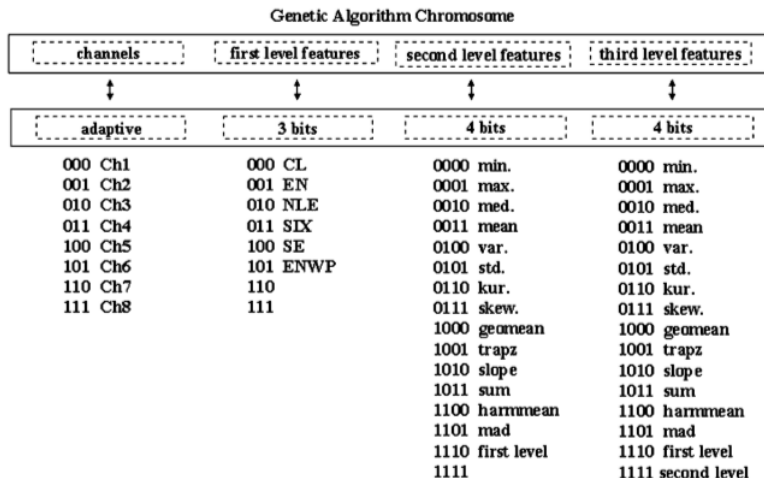


Figure: GA Chromosome

Classification

Probabilistic Neural Network (PNN) was used with the Genetic Algorithm (GA) selected features

Have a sensitivity of 62.5 percent with 90.5 percent specificity

Patient	IEEG Channel	Selected IEEG feature/channel for prediction	Specificity	Sensitivity	Prob. Error	Avg. Prediction Time (min)	False positives per hour
A	RT5-6	mean of median of curve length channel (LIF3-4)	100.00%	75.00%	0.01	5.56	0
B	RT2-3	max. of mean abs. deviation of energy channel (RT4-5)	85.00%	62.50%	0.13	3.25	0.36
C	RIF2-3	min. of median of curve length channel (LTI-2)	90.63%	62.50%	0.13	1.81	0.4
D	LIT1-2	minimum of sum of energy channel (LIT3-4)	86.25%	50.00%	0.09	3.2	0.35
AVERAGE VALUES			90.47%	62.50%	0.09	3.455	0.2775

Figure: Performance of D'allesandro

Fuzzy Techniques for Classification of Epilepsy Risk Level from EEG Signals by Narayan et al.

Data Collection

- 1 16 channels
- 2 Band pass filtered 0.5-70 Hz using a Butterworth filter
- 3 Epochs of 2 seconds
- 4 C++ and Matlab 5.3

DOI:10.1109/TENCON.2003.1273316

Fuzzy Techniques for Classification of Epilepsy Risk Level from EEG Signals by Narayan et al.

Features

- 1 Energy of the epoch
- 2 The number of positive and negative peaks exceeding a threshold
- 3 Number of spikes and sharp waves
- 4 Variance of each epoch

DOI:10.1109/TENCON.2003.1273316

- ➊ A fuzzier: converts real time values into fuzzy values
- ➋ An inference engine: applies a fuzzy reasoning mechanism
- ➌ A de-fuzzier: translates output into real time values
- ➍ A knowledge base: contains both an ensemble of fuzzy rules and database.

DOI:10.1109/TENCON.2003.1273316

- 1 The input variables: Energy, positive and negative peaks, spikes and sharp waves
- 2 The output variable: epilepsy risk level
- 3 Input: very low, low, medium, high, and very high
- 4 Output: normal, low risk, medium risk, high risk, very high risk

DOI:10.1109/TENCON.2003.1273316

Their quality was determined by three factors:

- ① Classification rate
- ② Classification delay
- ③ False alarm rate

DOI:10.1109/TENCON.2003.1273316

Details	Fuzzy Logic Classifier	Classifier after Optimization
Risk Level Classification rate (%)	50	80
Weighted Delay (s)	4	2.8
False alarm rate/set	0.2	0.1
Quality value	6.25	11.9

Figure: Performance of Narayan

DOI:10.1109/TENCON.2003.1273316

HUNTINGTON DISEASE

- ① Expansion in the Huntington gene causes death of the movement related areas of the brain
- ② Bylsma et al. states reduction in the alpha rhythm

Detection of subclinical brain electrical activity changes in Huntington's disease using artificial neural networks by De Tommaso et al.

- 1 3 patients, 7 subjects at risk, 13 normal subjects
- 2 Artifact-free epochs
- 3 Fast Fourier Transform Algorithm
- 4 Linear analysis with Fisher's Linear Discriminant (FLD) method, Likelihood Ratio Method (LRM), and also an Artificial Neural Networks (ANN) classifier
- 5 Results: The ANN correctly classified 11/13 patients and 12/13 normals.

[https://doi.org/10.1016/S1388-2457\(03\)00074-9](https://doi.org/10.1016/S1388-2457(03)00074-9)

The application of unsupervised artificial neural networks to the sub-classification of subjects at-risk of Huntington's Disease by Jervis et al.

- ➊ 11 Huntington's Disease (HD) patients, 21 at-risk subjects, equal number of controls
- ➋ Cognitive Negative Variation (CNV): Evoked Response Potential was examined for HD.
- ➌ Input data: The voltage and the duration of the CNV
- ➍ Classification: Kohonen and Adaptive Resonance Theory 2 (ART2) unsupervised artificial neural networks
- ➎ Results: Similar for both classifiers

Published in: IEE Colloquium
on Intelligent Decision Support
Systems and Medicine

Alzheimer is a common form of dementia and there is no cure. Early detection plays an important role to prevent some outcomes of the disease. Some features of Alzheimer include

- ① Increase of delta and theta power
- ② Decrease in alpha and beta activity
- ③ Decreased functional connectivity in the alpha and in the theta frequency bands (coherence)

Diagnostic value of quantitative EEG in Alzheimer's disease by Benny et al.

- 1 35 patients, 35 controls
- 2 Eyes closed and eyes opened
- 3 Electrodes with impedance lower than 5 Kohms
- 4 Signal was amplified, 0.3-40 Hz filtered
- 5 Artefact-free periods

[https://doi.org/10.1016/S0987-7053\(01\)00254-4](https://doi.org/10.1016/S0987-7053(01)00254-4)

Diagnostic value of quantitative EEG in Alzheimer's disease by Benny et al.

- 1 The average absolute power for 5 frequency bands
- 2 $\text{Theta}/\alpha + \beta_1$ (ratio r_1) and $\text{delta} + \text{theta}/\alpha + \beta_1 + \beta_2$ (ratio r_2) were calculated
- 3 Region of Convergence (ROC) curve being constructed to describe the performance (sensitivity and specificity)
- 4 Statistical analysis was performed
- 5 Conclusion: Increase in delta and theta power

[https://doi.org/10.1016/S0987-7053\(01\)00254-4](https://doi.org/10.1016/S0987-7053(01)00254-4)

"ROC analysis indicate that our parameters classified 40 percent of patients with a 100 percent specificity."

	<i>AD</i>	<i>Control</i>
T3T5O1		
$-r1 < 0.27$	62.8	100
$-r1 > 0.27$	37.2	0
(OCS* of $r1=0.50$)		
$-r2 < 0.45$	60.0	100
$-r1 > 0.45$	40.0	0
(OCS* of $r2=0.96$)		
T4T6O2		
$-r1 < 0.29$	65.7	100
$-r1 > 0.29$	34.3	0
(OCS* of $r1=0.52$)		
$-r2 < 0.45$	58.7	100
$-r2 > 0.45$	41.3	0
(OCS* of $r2=0.98$)		

Figure: Performance of Benny

Power Frequency and Wavelet Characteristics in Differentiating Between Normal and Alzheimer EEG by Yagneswaran et al.

- 1 9 Alzheimer Disease (AD) patients and 10 controls
- 2 9 channel EEG
- 3 The low pass at 0.5 and high-pass filter at 60Hz
- 4 Eyes-closed and eyes-open

DOI:10.1109/IEMBS.2002.1134380

Power Frequency and Wavelet Characteristics in Differentiating Between Normal and Alzheimer EEG by Yagneswaran et al.

- 1 Fourier power spectra comparative analysis
- 2 The statistical tests revealed no significant group differences thus sub-bands were calculated and theta, alpha, beta showed difference by t-test.
- 3 Input features 1: Three sub-bands, the relative power (RP), slower wave ratio (SWR)
- 4 daub5 wavelet
- 5 Input features 2: Averages of wavelet coefficients

DOI:10.1109/IEMBS.2002.1134380

- ① Power frequency input vectors had 9 spectral features
- ② Wavelet vectors had 7 features
- ③ Three-layer Learning Vector Quantization (LVQ) was designed with Neural Network toolbox from Matlab

Feature Set	Network Performance
Power Spectra Features	94.7% (18 out of 19)
Wavelet Coefficients	89.4% (17 out of 19)

Figure: Performance of Yagneswaran

DOI:10.1109/IEMBS.2002.1134380

Recurrent Neural Network and Wavelet Transform based Distinction Between Alzheimer and Control EEG by Petrosian et al.

- ① 3 Alzheimer patients and 3 controls
- ② Eyes-closed continuous 9 channel EEG recording
- ③ 2 min epochs were selected
- ④ Artefact free occipital channels were selected

DOI:10.1109/IEMBS.1999.804351

Recurrent Neural Network and Wavelet Transform based Distinction Between Alzheimer and Control EEG by Petrosian et al.

- 1 Wavelet pre-processing with daub4
- 2 Recurrent Neural Networks (RNN)
- 3 The training and testing were performed on both original EEG and wavelet filtered sub-signals

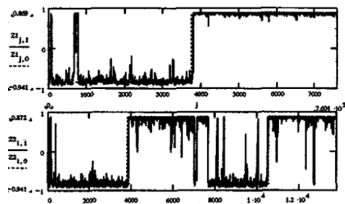


Figure: Performance of Petrosian

Automatic Recognition of Alzheimer's Disease with Single Channel EEG Recording by Cho et al.

- ① 16 AD patient
- ② 5 min eyes open
- ③ Artifact free segments
- ④ The Event Related Potentials (ERP) were acquired during the auditory oddball task
- ⑤ The subjects were instructed to count internally the number of the target tones

DOI:10.1109/IEMBS.2003.1280462

Automatic Recognition of Alzheimer's Disease with Single Channel EEG Recording by Cho et al.

- 1 30 s segments
- 2 88 power spectral measurements
- 3 2 chaotic features
- 4 10 ERP features
- 5 Chromosome as a string consisted of 35 constants

DOI:10.1109/IEMBS.2003.1280462

Automatic Recognition of Alzheimer's Disease with Single Channel EEG Recording by Cho et al.

- 1 The fitness value of a chromosome: The inverse of the sum of mean square errors of the Artificial Neural Networks (ANNs)
- 2 Maximum fitness valued chromosome for dominant feature set
- 3 35 dominant features: 24 spectral, 8 statistical, 1 nonlinear and 2 ERP features

$$Fitness = 1 / \sum_{i=1}^N mean(\sum_{j=1}^m (do_j - no_j)^2)$$

Figure: Fitness Value

DOI:10.1109/IEMBS.2003.1280462

- 1 For AD patients, 22 segments out of the 30 test segments
- 2 For the controls, 37 segments out of the 42 test segments were recognized correctly

Target NN output	Segments of AD patients	Segments of normal controls	Performance
AD	22	5	22/30 = 73%
Normal	8	37	37/42 = 88%
Total	30	42	59/72 = 81.9%

Figure: Performance of Cho

DOI:10.1109/IEMBS.2003.1280462

Evoked Potentials

- 1 Auditory Evoked Potential: EEG activity after auditory stimulus
- 2 Somatosensory Evoked Potential: EEG activity after somatosensory stimulus
- 3 Visual Evoked Potential: EEG activity after visual stimulus

- ➊ Attention Deficit Hyperactivity Disorder (ADHD) is basically lack of focus and extreme movement
- ➋ Bipolar Disorder is fundamentally extreme and sudden mood changes
- ➌ Some researches use changes in the energy level of EEG as a feature like Swartwood et al. which found a decrease in the alpha band of ADHD patients
- ➍ In another research, BMD and ADHD were differentiated by features such as fractal dimension, AR coefficients, and wavelet coefficients which had an accuracy 86.44 percent

Classification of ADHD and BMD patients Using Visual Evoked Potentials by Nazhvani et al.

- ❶ 12 ADHD, 12 BMD, 12 healthy subjects
- ❷ 22 electrodes according to 10-20 system
- ❸ Flashed by an array of LEDs

<https://doi.org/10.1016/j.clineuro.2013.08.009>

Classification of ADHD and BMD patients Using Visual Evoked Potentials by Nazhvani et al.

- 1 Wavelet based de-noising : sets coefficients below some threshold to zero
- 2 Synchronous averaging : to improve signal to noise ratio

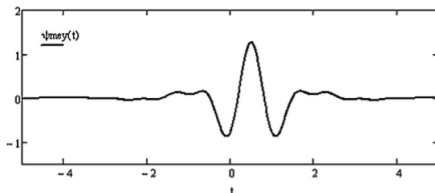


Figure: Meyer Wavelet

<https://doi.org/10.1016/j.clineuro.2013.08.009>

Classification of ADHD and BMD patients Using Visual Evoked Potentials by Nazhvani et al.

- 1 Channel O1 was selected
- 2 Amplitude and latency of P100 component as a feature
- 3 K-Nearest Neighbor (KNN) classifier : VEP has a multimodal distribution local based classifiers such as 1NN

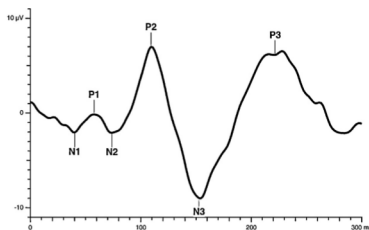


Figure: VEP

<https://doi.org/10.1016/j.clineuro.2013.08.009>

Classification of ADHD and BMD patients Using Visual Evoked Potentials by Nazhvani et al.

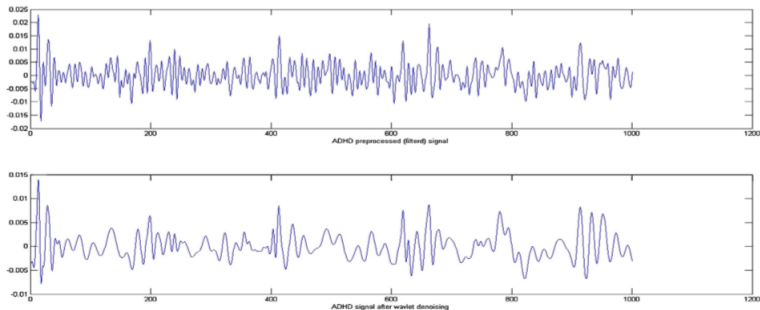


Figure: Wavelet Denoising of ADHD Signal

<https://doi.org/10.1016/j.clineuro.2013.08.009>

Classification of ADHD and BMD patients Using Visual Evoked Potentials by Nazhvani et al.

Features	Classification rate
Amplitude	87.75
Latency	84.69
Amplitude and Latency	92.85

Figure: Performance Nazhvani

<https://doi.org/10.1016/j.clineuro.2013.08.009>

BCI uses EEG to communicate with the computer to make it perform several tasks including cursor control, playing mental games, and robotic arms

It can be used to help people with neurodegenerative diseases such as Amyotrophic Lateral Sclerosis (ALS)

BCI Components

- 1 Signal acquisition
- 2 Signal preprocessing
- 3 Feature extraction and selection
- 4 Classification

Brain Computer Interface

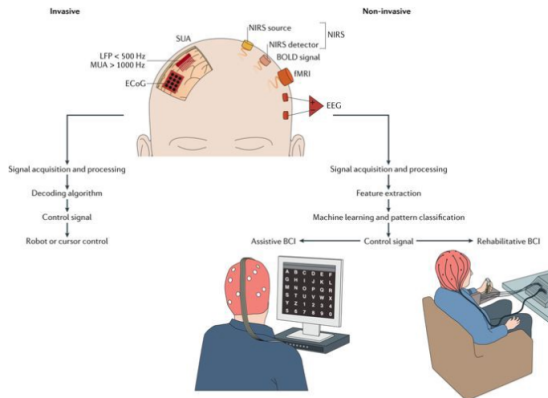


Figure: BCI

doi:10.1038/nrneuro.2016.113.

Separability of EEG Signals Recorded During Right and Left Motor Imagery Using Adaptive Autoregressive Parameters by Pfurtscheller et al.

- 1 4 subjects
- 2 Channels C3 and C4
- 3 Imagine either right or left hand movement
- 4 Computer was used for visual cue, as arrow direction

DOI:10.1109/86.712230

Separability of EEG Signals Recorded During Right and Left Motor Imagery Using Adaptive Autoregressive Parameters by Pfurtscheller et al.

- 1 Subject-specific band power
- 2 Imagination of hand movement is similar to Event-Related Desynchronization (ERD) patterns
- 3 In the first sessions, data were collected for the setup, no feedback
- 4 In the next sessions, feedback stimulus

DOI:10.1109/86.712230

Separability of EEG Signals Recorded During Right and Left Motor Imagery Using Adaptive Autoregressive Parameters by Pfurtscheller et al.

- 1 Subject-specific frequency components were selected by the Distinction Sensitive Learning Vector Quantization classifier (DSLQVQ)
- 2 A Learning Vector Quantization (LVQ) was used for the on-line classification.
- 3 For off-line classification, Recursive-Least-Squares (RLS) algorithm was used to estimate Adaptive AutoRegressive (AAR) parameter and
- 4 Linear Discriminant Analysis (LDA) used to calculate distance, if it is less than zero classification output is right, and otherwise classification is left.

DOI:10.1109/86.712230

Separability of EEG Signals Recorded During Right and Left Motor Imagery Using Adaptive Autoregressive Parameters by Pfurtscheller et al.

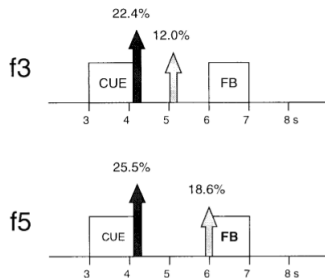


Figure: Performance of Pfurtscheller

A New Brain–Computer Interface Design Using Fuzzy ARTMAP by Palaniappan et al.

- 1 The EEG collected by Keirn and Aunon
- 2 2500 samples per channel
- 3 Power Spectral Density (PSD) values using the Wiener–Khinchine (WK) and AutoRegressive (AR) methods

DOI:10.1109/TNSRE.2002.802854

A New Brain–Computer Interface Design Using Fuzzy ARTMAP by Palaniappan et al.

- ① Baseline task: relax
- ② Math task: multiplication
- ③ Geometric figure rotation task: rotating three-dimensional block object
- ④ Mental letter composing task: compose a letter
- ⑤ Visual counting task: visualize numbers being written

DOI:10.1109/TNSRE.2002.802854

A New Brain-Computer Interface Design Using Fuzzy ARTMAP by Palaniappan et al.

The first method uses WK theorem

Second method AR spectral analysis with Burg method to overcome shortcoming of Yule-Walker approach(time consuming)

$$S(f) = T \sum_{k=-N}^N C(k) e^{-j2\pi k f T},$$

(a) WK Method

$$S(f) = \frac{\hat{\sigma}_p^2 T}{\left| \sum_{k=0}^p a_k e^{-j2\pi f k T} \right|^2}.$$

(b) Burg Method

DOI:10.1109/TNSRE.2002.802854

A New Brain-Computer Interface Design Using Fuzzy ARTMAP by Palaniappan et al.

- 1 Fuzzy ART-A receives input features representing the pattern
- 2 Fuzzy ART-B gives output features representing the target class
- 3 Inter ART module maps these two modules

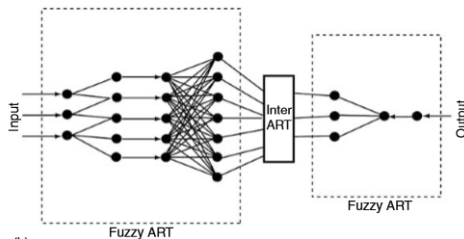


Figure: Fuzzy Structure

A New Brain-Computer Interface Design Using Fuzzy ARTMAP by Palaniappan et al.

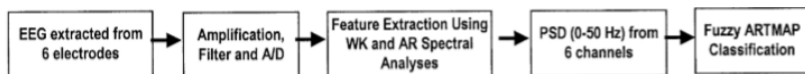


Figure: Flow Diagram of Palaniappan

DOI:10.1109/TNSRE.2002.802854

A New Brain-Computer Interface Design Using Fuzzy ARTMAP by Palaniappan et al.

Letter	Morse Code	Corresponding mental tasks
W	● — —	Letter, baseline, count, baseline, count, baseline
A	● —	Letter, baseline, count, baseline
T	—	Count, baseline
E	●	Letter, baseline
R	● — ●	Letter, baseline, count, baseline, letter, baseline

(a)

Figure: Morse Code and Mental Task for Water

DOI:10.1109/TNSRE.2002.802854

A New Brain-Computer Interface Design Using Fuzzy ARTMAP by Palaniappan et al.

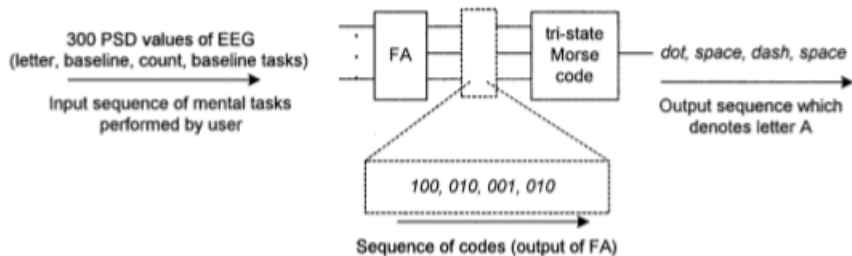


Figure: General Structure of the System

DOI:10.1109/TNSRE.2002.802854

A New Brain-Computer Interface Design Using Fuzzy ARTMAP by Palaniappan et al.

	WK-Parzen		WK-Tukey		AR	
	Task pair	FA %	Task pair	FA %	Task pair	FA %
Subject 1	Rotation, maths, baseline	95.02	Rotation, maths, baseline	85.83	Rotation, maths, baseline	90.83
Subject 2	Maths, baseline, letter	94.17	Maths, baseline, letter	92.00	Letter, counting, maths	95.84
Subject 3	Baseline, letter, count	96.67	Baseline, letter, count	96.50	Baseline, letter, count	99.00
Subject 4	Rotation, maths, count	91.83	Rotation, maths, count	90.00	Rotation, maths, baseline	89.00
Average		94.43		91.08		93.67

Figure: Performance of Palaniappan

DOI:10.1109/TNSRE.2002.802854

BCI Competition 2003—Data Set IV: An Algorithm Based on CSSD and FDA for Classifying Single-Trial EEG by Wang et al.

Classifying EEG during the preparation of self-paced tapping

- 1 Features: Bereitschaftspotential(BP)and Event-Related Desynchronization(ERD)
- 2 Feature Extraction: Common Spatial Sub-space Decomposition (CSSD)
- 3 Fisher Discriminant Analysis (FDA) can linearly project high dimensional data to one dimensional vector

DOI:10.1109/TBME.2004.826697

BCI Competition 2003—Data Set IV: An Algorithm Based on CSSD and FDA for Classifying Single-Trial EEG by Wang et al.

Classifying EEG during the preparation of self-paced tapping

- 1 First feature is derived from BP
- 2 Second feature is derived from ERD
- 3 Third feature is derived from BP
- 4 Classification: perceptron

DOI:10.1109/TBME.2004.826697

BCI Competition 2003—Data Set IV: An Algorithm Based on CSSD and FDA for Classifying Single-Trial EEG by Wang et al.

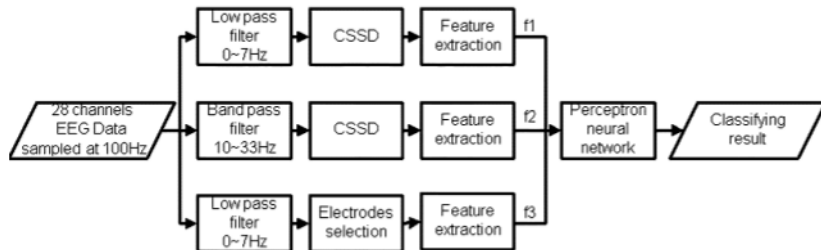


Figure: Flow Diagram of Wang

BCI Competition 2003—Data Set IV: An Algorithm Based on CSSD and FDA for Classifying Single-Trial EEG by Wang et al.

Features	Eigenvalues				
	e_1	e_2	e_3	e_4	e_5
f_1	82	51	53	55	52
f_2	84	77	70	61	59

Figure: Performance of Wang

84 percent accuracy

DOI:10.1109/TBME.2004.826697

A P300-Based Quantitative Comparison Between the Emotiv Epoch Headset and A Medical EEG Device by Duvinage et al.

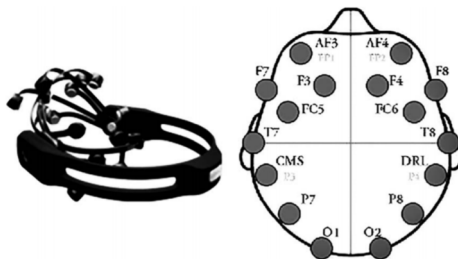


Figure: Emotiv EEG headset with electrode positions in 10/20 system

DOI:10.1002/asi.23904

A P300-Based Quantitative Comparison Between the Emotiv Epoch Headset and A Medical EEG Device by Duvinage et al.

- ① Portable
- ② Wireless
- ③ Fast setup
- ④ Low cost
- ⑤ High temporal resolution
- ⑥ Saline sensors

DOI:10.2316/P.2012.764-071

A P300-Based Quantitative Comparison Between the Emotiv Epoch Headset and A Medical EEG Device by Duvinage et al.

- 1 Medical EEG as Advanced Neuro Technology (ANT) with 512 Hz-128 channels
- 2 Emotiv Epoch with 128 Hz-14 channels
- 3 7 healthy male subjects
- 4 P300 Event Related Potential(ERP)
- 5 P300 has higher SNR than other activities of brain and muscles
- 6 4 state BCI for walking and sitting as low, medium, high speed and stop
- 7 32 Hz downsampling
- 8 Temporal high-pass filter, a spatial filter
- 9 Epoch averaging and Linear Discriminant Analysis (LDA) classifier
- 10 t-test was applied

A P300-Based Quantitative Comparison Between the Emotiv Epoch Headset and A Medical EEG Device by Duvinage et al.

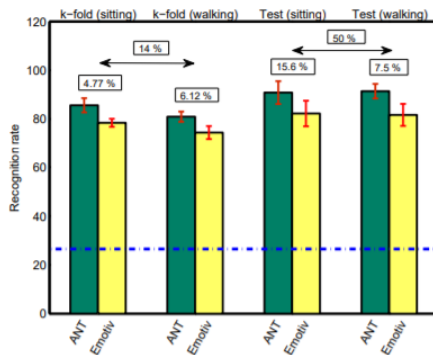


Figure: Performance Comparison of Emotiv and ANT

A P300-Based Quantitative Comparison Between the Emotiv Epoch Headset and A Medical EEG Device by Duvinage et al.

- 1 Emotiv was worse than the ANT
- 2 SNR was worse in the Emotiv compared ro ANT
- 3 "...although less good than the ANT system in average.Emotiv can be used in non-critical applications such as games"

DOI:10.2316/P.2012.
764-071

Towards Low-Cost P300-Based BCI Using Emotiv Epoc Headset by Liu et al.

- ① Aim: evaluate performance of Emotiv on P300
- ② 3 males 2 females
- ③ 25 English letters as a 5x5 matrix
- ④ Task: count internally each time letter occurs on screen
- ⑤ Matlab and EEGLAB
- ⑥ Preprocessing: 0.1-30 Hz bandpass filter, downsampling, windowing
- ⑦ Feature: P300 amplitude
- ⑧ Classification: Support Vector Machine (SVM)

DOI:10.1007/
978-3-319-66939-7_20

Towards Low-Cost P300-Based BCI Using Emotiv Epoc Headset by Liu et al.

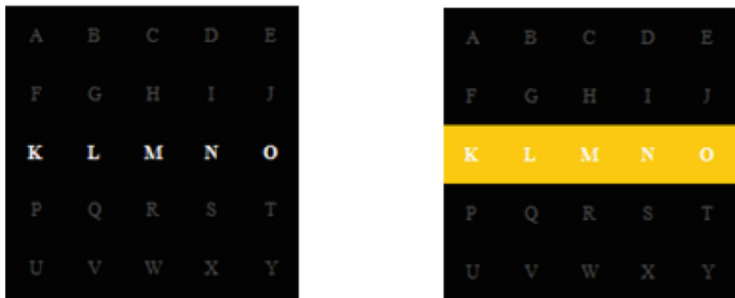


Figure: Emotiv Paradigm I and II

DOI:10.1007/
978-3-319-66939-7_20

Towards Low-Cost P300-Based BCI Using Emotiv Epoc Headset by Liu et al.

Participants	Accuracy (%)		P300 amplitude (μ V)	
	Paradigm I	Paradigm II	Paradigm I	Paradigm II
S1	74.29	78.57	4.76	5.02
S2	78.57	80.71	4.04	4.72
S3	72.86	69.29	3.91	4.33
S4	76.43	79.29	4.38	4.89
S5	75.71	77.14	5.26	5.72
Mean	75.57	77.01	4.47	4.94

Figure: Performance of Emotiv

Thank
You